Journal of Cerebral Blood Flow & Metabolism (2015) 35, 367–370

www.jcbfm.com

BRIEF COMMUNICATION

Mapping functional connectivity using cerebral blood flow in the mouse brain

Karla M Bergonzi[1], Adam Q Bauer[2], Patrick W Wright[1] and Joseph P Culver[1,2,3]

Brain function can be assessed from resting-state functional connectivity (rs-fc) maps, most commonly created by analyzing the dynamics of cerebral hemoglobin concentration. Here, we develop the use of Laser Speckle Contrast Imaging (LSCI) for mapping rs-fc using cerebral blood flow (CBF) dynamics. Because LSCI is intrinsically noisy, we used spatial and temporal averaging to sufficiently raise the signal-to-noise ratio for observing robust functional networks. Although CBF-based rs-fc maps in healthy mice are qualitatively similar to simultaneously-acquired [HbO_2]-based maps, some quantitative regional differences were observed. These combined flow/concentration maps might help clarify mechanisms involved in network disruption during disease.

Journal of Cerebral Blood Flow & Metabolism (2015) **35,** 367–370; doi:10.1038/jcbfm.2014.211; published online 10 December 2014

Keywords: brain imaging; cortical mapping; intrinsic optical imaging; neurovascular coupling

INTRODUCTION

In humans, functionally-related brain networks exhibit temporally-coherent patterns of spontaneous activity and show resting-state functional connectivity (rs-fc) as measured by magnetic resonance imaging (fcMRI).[1] The same phenomena has been observed in rats with fcMRI and recently in the mouse cortex with Optical Intrinsic Signal (fcOIS) imaging.[2,3] However, interpreting fc disruptions from disease is potentially complicated by regionally-altered neurovascular coupling.[4] Supplementing the blood oxygenation level-dependent signal of fcMRI, or fluctuations in hemoglobin concentration of fcOIS with cerebral blood flow (CBF), could provide a more comprehensive assay that potentially helps clarify disease-related mechanisms involved in network disruption.

Recent studies have combined arterial spin labeling measures of CBF with the blood oxygenation level-dependent measures to provide multiple contrasts in human fc analyses.[5] However, extending these MRI techniques (blood oxygenation level-dependent and arterial spin labeling) to fcMRI in mice is difficult due to a number of challenges related to acquiring data with a high signal-to-noise ratio (SNR). In mice, an alternate optical technique, Laser Speckle Contrast Imaging (LSCI), can be used to measure CBF over the entirety of the superficial mouse cortex with reasonably high spatial ($< 200\,\mu$m) and temporal (< 0.01 s) resolution.[6] However, it is not clear that the SNR of LSCI data is sufficient for measuring the small spontaneous changes in CBF during resting-state conditions. In traditional event-related neuroimaging studies, block averaging over many trials reduces competing noise sources, but rs-fc measures require high instantaneous SNR for accurately measuring temporal correlations in spontaneous brain activity. Here, we analyze the SNR of spontaneous LSCI measurements and present fc maps in mice using fcLSCI. These CBF-derived fc maps are compared with those concurrently recorded with fcOIS.

MATERIALS AND METHODS

Animal Preparation

All animal studies were approved by the Washington University School of Medicine Animal Studies Committee (protocol #20130217) under guidelines and regulations consistent with the Guide for the Care and Use of Laboratory Animals, Public Health Service Policy on Humane Care and Use of Laboratory Animals, and the Animal Welfare Act and Animal Welfare Regulations. Male Swiss Webster mice ($n = 5$, 6 to 10 weeks of age, 28 to 32 g, Harlan Laboratories, Indianapolis, IN, USA) were anesthetized with an intraperitoneal injection of Ketamine-Xylazine (86.9 mg/kg Ketamine and 13.4 mg/kg Xylazine) and fixed in a stereotactic frame. The scalp was reflected about midline to expose the intact skull to which mineral oil was periodically applied to prevent drying. The body temperature of the mouse was maintained at 37°C *via* feedback from a rectal probe (TCII, Cell MicroControls, Norfolk, VA, USA). To collect resting-state and evoked-response data on each mouse, which require longer imaging times than a bolus of ketamine-xylazine would allow, after injection mice were infused with a saline-ketamine cocktail (34.8 mg/kg per hour ketamine).

Imaging

The experimental setup combined the fcOIS and LSCI systems as previously developed.[2,6] Interleaved OIS and LSCI were acquired (at 16 Hz each) with a single EMCCD camera (Andor iXon^{EM} 897, Belfast, UK, 512×512 pixels, pixel size $16\,\mu\text{m} \times 16\,\mu$m) and lens (Vivitar Series 1, 85 mm, Edison, NJ, USA) at full spatial resolution (without binning) (Figure 1A). The incident angle of the LEDs (472 ± 30 nm, 628 ± 32 nm, LCS-0470-15-22, LCS-0625-03-22, Mightex Systems, Pleasanton, CA, USA) and laser (690 nm, 39 mW diode, Thorlabs HL6738MG, Newton, NJ, USA) illuminating the skull was 30° to the optical axis of the lens. The image integration

[1]Department of Biomedical Engineering, Washington University in St Louis, St Louis, Missouri, USA; [2]Department of Radiology, Washington University in St Louis, St Louis, Missouri, USA and [3]Department of Physics, Washington University in St Louis, St Louis, Missouri, USA. Correspondence: Professor JP Culver, Department of Radiology, Washington University School of Medicine, 660 South Euclid Avenue, Campus Box 8225, St Louis, MO 63110, USA.
E-mail: culverj@mir.wustl.edu
This study was supported by the National Institutes of Health (R01NS078223 (JPC), P01NS080675 (JPC), and K25NS083754 (AQB)), Washington University's Imaging Science Pathway (PWW), and Washington University's Olin Fellowship (KMB).
Received 29 April 2014; revised 24 October 2014; accepted 27 October 2014; published online 10 December 2014

times were 30 ms for each OIS wavelength and 10ms for LSCI, and the laser speckle pattern was collected using an f-number = 5.6 and magnification = 1x.[6]

Fifteen minutes of resting-state data were collected in each mouse. Cortical responses in left somatosensory barrel cortex were elicited by positioning the mouse's whiskers through a mesh screen, 1cm from the whisker base. A block design was used ($n = 24$ blocks), where each 50-second stimulus block consisted of 10 seconds of stimulation followed by 40 seconds of recovery. During stimulation, the mesh deflected the whiskers 1mm laterally at 3 Hz.[7]

Data Analysis and Statistics

Speckle contrast (SC) was calculated by $SC = \sigma(I)/ < I >$, the standard deviation, σ, divided by the mean of the intensity measurements, I, over a sliding 5x5 region of pixels following the previous publications.[8] Speckle contrast images were converted into a relative index of instantaneous CBF using the approximation that $iCBF = 1/SC^2$.[9] The OIS data were converted to changes in hemoglobin concentration as previously described.[2] The full-resolution CBF and OIS image sequences (512 × 512 pixels) were spatially binned using an 8 × 8 kernel to 64x64 pixels to reduce noise and data set size.

The FC analysis was performed on 15 minutes of preprocessed CBF and $[HbO_2]$ data for each mouse by applying a bandpass temporal filter (0.009 to 0.08Hz) and regressing the average signal from each hemisphere.[10] Seed placement was determined from anatomy (a coregistered Paxinos anatomical atlas[2]), and seed time traces were calculated by averaging the time traces of each pixel within 0.25 mm of a seed locus. The FC maps were created by calculating the correlation coefficient between each seed's time trace and those in every brain pixel. Bilateral correlations were determined by correlating a seed-based time trace with that of its contralateral homolog. Pearson r-values were converted to Fisher Z-measures before group averaging, and all statistical analyses of FC values were performed using a two-tailed Student's t-test.

RESULTS

To evaluate the feasibility of mapping rs-fc with LSCI, we used stimulated activity to estimate the spontaneous CBF activity in a single mouse. Because resting-state fluctuations in $[HbO_2]$ are ~1%,[2] the ratio of CBF and $[HbO_2]$ provides an estimate of the expected spontaneous CBF changes (Figure 1B). To improve SNR, data were temporally downsampled to 1Hz and spatially smoothed using a Gaussian kernel (full width at half maximum (FWHM) = 8 pixels, 1.25 mm). After block averaging the whisker-stimulation data ($n = 24$ trials), the percent change of the hemodynamic response measured: $[HbO_2]$ = 4%, [HbR] = −2%, [HbT] = 2%, and CBF = 6%, which are comparable to published results.[7,11] The measured ratio of $\Delta CBF/\Delta[HbO_2]$ is 1.5, and because spontaneous $\Delta[HbO_2]$ is ~1%, spontaneous ΔCBF is expected to be ~1.5%.

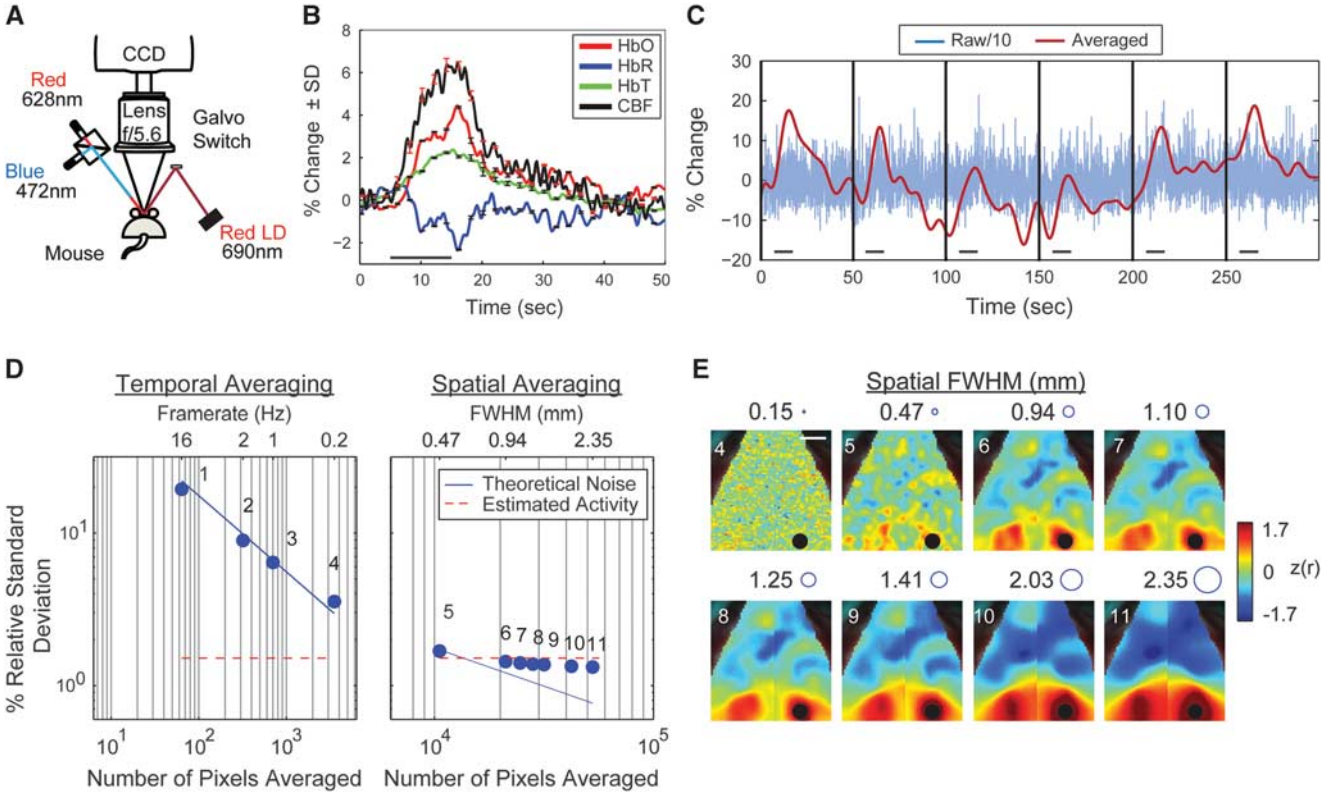

Figure 1. Laser Speckle Contrast Imaging (LSCI) can measure single-trial cerebral blood flow (CBF) activations with temporal and spatial averaging. (**A**) System setup for simultaneous Optical Intrinsic Signal (OIS) and LSCI imaging. (**B**) Averaged mechanical whisker pad activations of $[HbO_2]$, [HbR], [HbT], and CBF ($n = 24$). Stimulus occurred during time 5 to 15 seconds as marked by the black horizontal line. Error bars are ± the standard deviations across trials. (**C**) Blue: Time trace of the raw (16 Hz) percent change in CBF for six activations, separated by black vertical bars. Red: After temporal and spatial averaging (frame rate = 1Hz and full width at half maximum (FWHM) = 1.25 mm), responses to single stimulations can be seen in the CBF data. The magnitude of the raw trace has been divided by 10 to fit on the same scale as the averaged trace. (**D**) The effect of temporal (left) and spatial (right) averaging on the relative standard deviation of CBF data. The blue line shows the theoretical reduction in noise due to averaging pixels, while the red dotted line shows the estimated spontaneous CBF activity. The numbers of the dots correspond to the maps in (**E**). (**E**) Effect of spatial averaging on the functional connectivity (fc) map for the Right Visual seed (black circle). The circles next to the kernel size show the FWHM to scale. The 2-mm white scale bar in the top left map applies to all maps in (**E**).

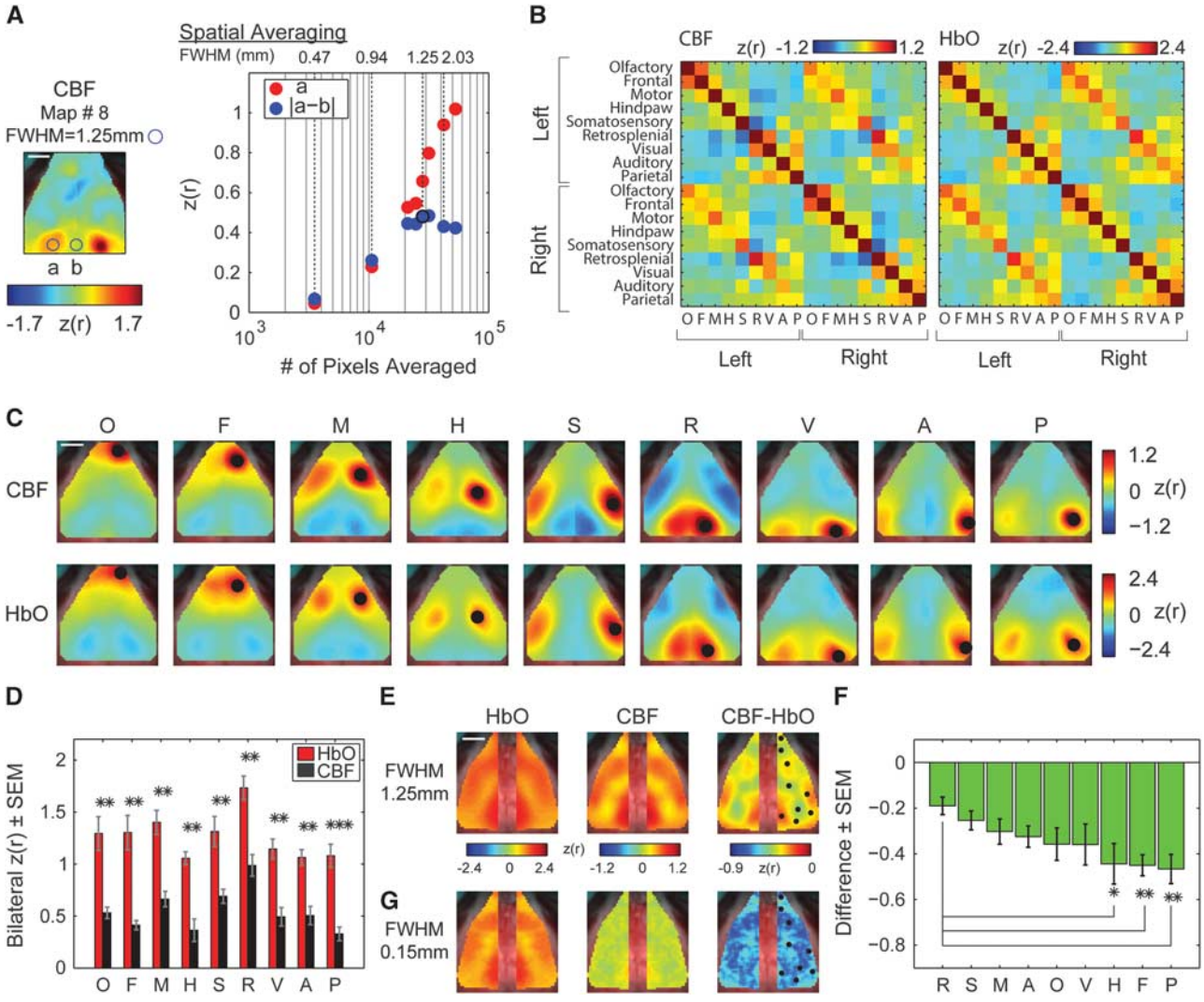

Figure 2. Laser Speckle Contrast Imaging (LCSI) can be used to analyze the temporal synchrony between regional cerebral blood flow (CBF). (**A**, left panel) The effect of spatial averaging on the topography of CBF-based fc patterns was optimized by examining the difference between known functional connections of right visual cortex (left homotopic visual cortex, circle 'a') and a nonfunctionally-connected brain region proximal to those locations (midline, circle 'b'). Blue circle shows the full width at half maximum (FWHM) to scale and applies to (**A**, **C**, and **E**). The scale bar represents 2 mm. (**A**, right panel) In general, smoothing increases signal-to-noise ratio (SNR) in measurements of fc between right and left visual cortex (red circles). However, smoothing begins to decrease the difference between circles 'a' and 'b' (blue circles), with kernel sizes $\geq$2.03 mm FWHM. Kernel sizes of 1.25 to 1.41 mm FWHM (maps 8 and 9 in Figure 1E) show the largest difference, optimizing the topography of the fc pattern. Using an optimal smoothing parameter (FWHM = 1.25 mm), (**B**) the correlation matrices, (**C**) functional connectivity (fc) maps, and (**E**) bilateral maps of concurrently recorded CBF and [HbO_2] ($n = 5$ mice) are qualitatively similar, (**D**) however the CBF-based bilateral values are significantly lower than those of [HbO_2] (*$P < 0.05$, **$P < 0.01$, ***$P < 0.001$). (**E**) The difference between the CBF and [HbO_2] bilateral maps (CBF – [HbO_2] for FWHM = 1.25 mm) shows that the retrosplenial, motor, and somatosensory seeds have small differences while (**F**) the parietal, frontal, and hindpaw seeds have significantly larger differences between contrasts when compared with the difference in the retrosplenial seed. Seeds are shown as black circles in the right column. (**G**) The bilateral [HbO_2] map looks similar with large and small smoothing (**E** and **G**, respectively) while the CBF map with small smoothing does not show any structure, leading to no significant region-dependent differences.

Noise in the CBF measurement was estimated by examining the time course of the stimulation without block averaging (Figure 1C) to determine whether LSCI has sufficient SNR for reporting spontaneous neural activity. Without any temporal averaging (full frame rate = 16Hz) and with 0.12 mm spatial averaging, the standard deviation of the measured spontaneous CBF activity was SD_iCBF = 44.2% (Figure 1C, blue line). After temporally averaging to 1 Hz and spatial smoothing (Gaussian kernel, FWHM = 8 pixels, 1.25 mm), responses to individual stimuli (~6%) can be clearly observed above background (~1.5%, Figure 1C, red line). This result suggests that similar spatio-temporal averaging may reduce LSCI noise enough to measure resting-state fluctuations.

Noise reduction in CBF measurements was evaluated by analyzing a sequence of temporal and spatial filters applied to a 5-minute resting-state CBF data set ($n = 1$ mouse, Figure 1D). With increased temporal smoothing (Figure 1D, points 1 to 4), the SD_iCBF decreases following theoretical expectations from averaging a Gaussian noise source (SD ~ $1/\sqrt{N}$, where N is the number of pixels averaged in time). By further smoothing the 0.2 Hz data with spatial averaging (Figure 1D, points 5 to 11), the

SD_iCBF levels out at ~1.5% (Figure 1D, red line) and indicates that the SD_iCBF is now largely attributable to resting-state fluctuations instead of LCSI measurement noise.

Next, we evaluated how the same set of spatial filters affected the seed-based correlation maps (Figure 1E) to test the feasibility of mapping rs-fc with averaged LSCI. While modest amounts of spatial averaging (using the smallest spatial filters) do not produce sufficient SNR for measuring fc patterns, for spatial filters ≥ 0.94 mm, bilaterally symmetric spatial structures begin to emerge in fcLSCI maps (Figure 1E) that topographically resemble those observed with fcOIS.[2,10]

For quantifying the optimal spatial smoothing parameters (Figure 2A), the correlation coefficient and a measure of the resultant spatial connectivity profile were tracked as a function of smoothing amount. With increased averaging, the correlation value of the contralateral seed (Figure 2A, circle A) continuously increased which might suggest that more smoothing would be superior. However, increased smoothing also reduces the spatial specificity of a seed's fc map (Figure 1E). Optimal smoothing was determined when the difference between the bilateral fc value of visual cortex and an uncorrelated region between the two seeds no longer increased with increased smoothing (FWHM $\geq$ 2.03mm, Figure 2A, circle B).

The fcLSCI maps were averaged across five mice using smoothing parameters within the optimal range (FWHM = 1.25 mm, corresponding to smoothing parameters in Figure 2A, map #8). Although the fcLSCI correlation matrices (Figure 2B), seed-based fc maps (Figure 2C), and bilateral fc maps (Figure 2E) appear to have qualitatively similar structure to those calculated using [HbO_2], the bilateral seed-to-seed correlation coefficients are significantly smaller (Figure 2D, pO = 0.0068, pF = 0.0045, pM = 0.0011, pH = 0.0012, pS = 0.0087, pR = 0.0013, pV = 0.00011, pA = 0.0014, and pP = 0.00009). The spatial pattern of the bilateral fc structure in the CBF-based maps was explored by using each pixel as a seed and smoothing at both FWHM = 1.25 mm (Figure 2E) and FWHM = 0.15 mm (Figure 2G). Although the bilateral fc maps are similar for fcOIS at both small and large smoothing (Figures 2E and 2G, first column), quantitative comparisons of bilateral fcLSCI and fcOIS maps reveal significant regional differences. In particular, the differences between the fcLSCI and fcOIS correlation values (fcLSCI-fcOIS, Figure 2E and 2G, third column) in parietal, frontal, and hindpaw areas were statistically greater than the difference in the Retrosplenial cortex. The difference in the frontal and parietal regions remains significant after accounting for multiple comparisons (Figure 2F, (pR = 1, pS = 0.29, pM = 0.13, pA = 0.06, pO = 0.08, pV = 0.14, pH = 0.04, pF = 0.02, and pP = 0.008); these differences were not seen in the data smoothed with the small kernel.

DISCUSSION

This study shows that rs-fc maps can be created from CBF data. Although LSCI measurements are inherently noisier than OIS measurements, a combination of temporal and spatial averaging sufficiently reduces measurement noise for observing evoked brain activity from a single stimulus presentation (Figure 1C) and correlations in spontaneous activity (Figure 2). Although fcLSCI maps qualitatively agree with fcOIS maps,[2] there are regional differences (Figure 2). In general, correlation strengths are lower in CBF measurements compared with those from OIS. While there could still be residual noise in fcLSCI measurements not overcome by averaging, this noise would most likely be relatively even over the field-of-view as our averaging strategy was performed over that same field-of-view. In principle, LSCI noise would manifest as a uniform reduction in connectivity strength over the brain; however, we observe region-dependent differences in CBF-derived fc measures (Figures 2E and 2F). These differences are likely due to regional physiologic differences in the temporal coherence of CBF. Possible sources for this physiologic variance might include spatial differences in hemodynamic response functions, neurovascular coupling, or nonstationary responses.[12]

Future studies that involve more comprehensive comparisons between the hemodynamic variables and manipulations of baseline blood flow (e.g., with hypercapnia) or brain state (e.g., anesthesia dose, anesthetic type,[13] or awake imaging) will be required to gain further insight into the etiology of the regional differences between fcLSCI and fcOIS. Additionally, changes to the experimental setup could optimize the LSCI data quality including using a higher frame rate or pixel counts to further improve the SNR of LSCI.

Combining CBF-based resting-state measurements with those collected with fcOIS imaging will provide a more comprehensive physiologic assessment that might be advantageous in studies of disease progression where neurovascular coupling becomes altered.[4,14] In addition, fcOIS measurements can be combined with CBF measurements to calculate dynamic metabolic measures (e.g., cerebral metabolic rate of oxygen) and Grubb coefficients that, in principal, provide more direct measures of brain activity and brain energetics than [Hb] measurements alone.

DISCLOSURE/CONFLICT OF INTEREST

The authors declare no conflict of interest.

REFERENCES

1 Biswal B, Yetkin FZ, Haughton VM, Hyde JS. Functional connectivity in the motor cortex of resting human brain using echo-planar MRI. *Magn Reson Med* 1995; **34**: 537–541.
2 White BR, Bauer AQ, Snyder AZ, Schlaggar BL, Lee J-M, Culver JP. Imaging of functional connectivity in the mouse brain. *PLoS ONE* 2011; **6**: e16322.
3 Pawela CP, Biswal BB, Cho YR, Kao DS, Rupeng L, Jones SR *et al.* Resting-state functional connectivity of the rat brain. *Magn Reson Med* 2008; **59**: 1021–1029.
4 Iadecola C. Neurovascular regulation in the normal brain and in Alzheimer's disease. *Nat Rev Neurosci* 2004; **5**: 347–360.
5 Viviani R, Messina I, Walter M. Resting state functional connectivity in perfusion imaging: correlation maps with BOLD connectivity and resting state perfusion. *PLoS ONE* 2011; **6**: e27050.
6 Dunn AK, Bolay H, Moskowitz MA, Boas DA. Dynamic imaging of cerebral blood flow using laser speckle. *J Cereb blood flow Metab* 2001; **21**: 195–201.
7 Gerrits RJ, Raczynski C, Greene AS, Stein EA. Regional cerebral blood flow responses to variable frequency whisker stimulation: an autoradiographic analysis. *Brain Res* 2000; **864**: 205–212.
8 Briers JD, Webster S. Laser Speckle Contrast Analysis (LASCA): a nonscanning, full-field technique for monitoring capillary blood flow. *J Biomed Opt* 1996; **1**: 174–179.
9 Cheng H, Duong TQ. Simplified laser-speckle-imaging analysis method and its application to retinal blood flow imaging. *Opt Lett* 2007; **32**: 2188–2190.
10 Bauer AQ, Kraft AW, Wright PW, Snyder AZ, Lee J-M, Culver JP. Optical imaging of disrupted functional connectivity following ischemic stroke in mice. *Neuroimage* 2014; **99C**: 388–401.
11 Dunn AK, Devor A, Bolay H, Andermann ML, Moskowitz MA, Dale AM *et al.* Simultaneous imaging of total cerebral hemoglobin concentration, oxygenation, and blood flow during functional activation. *Opt Lett* 2003; **28**: 28–30.
12 Cabral J, Hugues E, Sporns O, Deco G. Role of local network oscillations in resting-state functional connectivity. *Neuroimage* 2011; **57**: 130–139.
13 Franceschini MA, Radhakrishnan H, Thakur K, Wu W, Ruvinskaya S, Carp S *et al.* The effect of different anesthetics on neurovascular coupling. *Neuroimage* 2010; **51**: 1367–1377.
14 Lacalle-Aurioles M, Mateos-Pérez JM, Guzmán-De-Villoria JA, Olazarán J, Cruz-Orduña I, Alemán-Gómez Y *et al.* Cerebral blood flow is an earlier indicator of perfusion abnormalities than cerebral blood volume in Alzheimer's disease. *J Cereb blood flow Metab* 2014; **34**: 654–659.